Synthetic Aperture Sonar Imaging via One-Way Wave Equations

Quyen Huynh* Kazufumi Ito†

June 23, 2008

Abstract

We develop an efficient algorithm for Synthetic Aperture Sonar imaging based on the one-way wave equations. The algorithm utilizes the operator-splitting method to integrate the one-way wave equations. The well-posedness of the one-way wave equations and the proposed algorithm is shown. A computational result against real field data is reported and the resulting image is enhanced by the BV-like regularization.

1 Introduction

In this paper we discuss the migration method based on one-way wave equations [1, 2] for Synthetic Aperture Sonar (SAS) imaging [3]. The one-way wave equation integrates the data within a given angle and minimizes the undesirable effects of unwanted reflections. Efficient and stable integration methods of the one-way wave equation based on the operator splitting method are used to develop a fully discretized algorithm. The stability analysis and the required operation count of the proposed algorithm are given. We test the proposed method for real field data and report our SAS imaging results. We also discuss the image enhancement method for the resulting images, based on BV-like regularization technique [5].

In side-scan (side-looking) sonar systems a platform containing a moderately large real aperture antenna travels along a rectilinear path in the along track direction and periodically transmits a pulse at an angle that is perpendicular to the platform path. These systems produce strip-map (SAS) images . A strip-map image is built up as follows; the imaging system operates such that the echoes from the current pulse are received before the next pulse is transmitted. As these echoes are received they are demodulated, pulse compressed, and detected (only the magnitude information is retained). Each detected pulse produces a

*Naval Surface Warfare Center - Panama City FL, research partially supported by the US Office of Naval Research under N00014-06-WX20559.

†Center for Research in Scientific Computation, Department of Mathematics, North Carolina State University; research partially supported by the US Office of Naval Research under N00014-06-1-0067.

range line of the real aperture image. As the platform moves these range lines are displayed next to each other at pixel spacings that scale relative to the along track spacing of the pulses $\Delta x = v_p \tau$ where v_p is the platform velocity and τ is the pulse repetition period. The final image is essentially a raster scan of a strip of the sea floor, hence the name "strip-map image". Synthetic aperture imaging is a coherent imaging technique that exploits the extra information available in the phase of the real aperture data. We adopt the Stop and Go model; a point source radiates at time $t = 0$, a spherical wave that reaches the sampling points after different time intervals. If the source is placed at (x_0, z_0) the time $t(x, x_0, z_0)$ at which the wave arrives at the sampling point (x, z) is:

$$t(x, z, x_0, z_0) = \frac{2}{c}\sqrt{(x - x_0)^2 + (z - z_0)^2}.$$

The field d due to a distribution $s(x, z)$ of source emitting at $t = 0$ can be expressed by

$$\hat{d}(x, z, \omega) = \frac{1}{4\pi} \int s(x', z') \frac{e^{-j(2\omega/c)\sqrt{(x-x')^2+(z-z')^2}}}{\sqrt{(x - x')^2 + (z - z')^2}}\, dx' dz'$$

where $\hat{d}$ is the Fourier transform (in time) of the signal d. SAS measures

$$\mathrm{SAS}(x, t) = d(x, z = 0, t)$$

along the sonar path $(x, z = 0) = \Gamma$.

Thus, SAS imaging is formulated as a linear inverse problem;

Problem: Reconstruct $s(x, z)$ from SAS data $\mathrm{SAS}(x, t)$.

Among a number of algorithms [3, 4, 6] and reference therein, which have been developed for Problem the frequency domain ω-k method based on Stolt's map [3, 7, 1] is the most efficient and accurate method. As will be discussed in Section 4 it has certain limitations, especially it assumes the homogeneous scattered media. The proposed method can incorporate inhomogeneous media and has additional capabilities, (see Section 4).

An outline of the paper is as follows. In Section 2 we describe a geometric migration method based on one-way wave equations for reconstructing s. A noble algorithm using the integration of the one-way wave equations based on the operator-splitting method is developed and its stability and complexity are analyzed in Section 3. In Section 3 we list advantages of the proposed method comparing to the ω-k method. The image enhancement technique based on the BV-type reguralization is discussed in Section 4. In Section 5 we present a test against real field data, provided by the Naval Surface Warfare Center-Panama City, Florida and a comparison with the ω-k method.

2 Geometric Migration

We construct an approximating solution based on the geometrical migration via the one-way wave equations. Let

$$A(k_x, \omega) = \mathcal{F}_{x,t}\,\mathrm{SAS}(x, t).$$

Assume the plane wave extrapolation

$$D(k_x, k_z, \omega) = A(k_x, \omega) exp(j(\omega t + k_x x + k_z z))$$

with

$$\omega^2 = \frac{c^2}{4}(k_x^2 + k_y^2).$$

Then the inverse Fourier transform of D

$$\tilde{d}(x, z, t) = \frac{1}{(2\pi)^3} \int D(k_x, k_z, \omega) dk_x dk_z d\omega$$

satisfies the wave equation

$$\frac{4}{c^2}\frac{\partial^2 \tilde{d}}{\partial t^2} = \frac{\partial^2 \tilde{d}}{\partial x^2} + \frac{\partial^2 \tilde{d}}{\partial z^2} \tag{3}$$

with the boundary condition at $z = 0$

$$\tilde{d}(x, 0, t) = \mathrm{SAS}(x, t)$$

and

$$\tilde{d}(x, z, T) = 0 \text{ and } \frac{\partial \tilde{d}}{\partial t}(x, z, T) = 0.$$

Wave equation based migration integrates the wave equation (3) backward in time to obtain an approximation $\tilde{s}$ of distribution s as;

$$\tilde{d}(x, z, 0) = \tilde{s}(x, d).$$

SAS data is created by integrating over the beam-width of the sensor. The radiation pattern of any dimension (width or length) of an aperture has an angular dependence that is referred to as the beam pattern of the aperture. Beam patterns are frequency dependent and have beam-widths given by the 3dB response of their main lobes; $\theta = \alpha_w \frac{c}{fD}$ where D is the length of the aperture and f are the frequency of the signal that the aperture is transmitting or receiving. The term α_w is a constant reflecting the main lobe widening due to weighting of the aperture illumination function. For example $f = 120$kHz and $D = 0.04$m and $\alpha_w = 1$ gives $\theta = 17.9$ degrees Thus, in order to speed-up the wave equation based algorithm and

minimize the undesirable effects of unwanted reflections we use the (15 degree) one-way wave equation based on

$$k_z = k\sqrt{1-\left(\frac{k_x}{k}\right)^2} \sim k\,(1-\frac{1}{2}(\frac{k_x}{k})^2) \tag{4}$$

where $k = 2\omega/c$ and we assumed $|k_x/k| << 1$. In time domain (4) is equivalently written as

$$\frac{4}{c^2}\frac{\partial^2 u}{\partial t^2} + \frac{2}{c}\frac{\partial^2 u}{\partial z \partial t} = \frac{1}{2}\frac{\partial^2 u}{\partial x^2}. \tag{5}$$

with

$$u(t,x,0) = \mathrm{SAS}(x,t),\ x \in \Gamma.$$

An advantage of the method is that it allows one to have a specified variable wave speed $c = c(x,z)$ of media. The corresponding method for the polar and cylindrical geometry is given as

Polar coordinate

$$\frac{4}{c^2}\frac{\partial^2 u}{\partial t^2} + \frac{2}{c}\frac{\partial^2 u}{\partial \nu \partial t} = \frac{1}{2}\frac{1}{r}\frac{\partial^2 u}{\partial \theta^2}.$$

Cylinder

$$\frac{4}{c^2}\frac{\partial^2 u}{\partial t^2} + \frac{2}{c}\frac{\partial^2 u}{\partial \nu \partial t} = \frac{1}{2}(\frac{1}{r}\frac{\partial^2 u}{\partial \theta^2} + \frac{\partial^2 u}{\partial z^2}).$$

We can derive the wide angle one-way wave equation based on the rational approximation

$$k_z = k\sqrt{1-\left(\frac{k_x}{k}\right)^2} \sim k\,(1-\frac{\alpha(k_x/k)^2}{1-\beta(k_x/k)^2}) \tag{6}$$

we have

$$k_z(k - \frac{\beta}{k}k_x^2) = k^2 - (\alpha+\beta)k_x^2$$

The differential form is given by

$$\frac{4}{c^2}\frac{\partial^2 u}{\partial t^2} + \frac{\partial}{\partial z}\left(\frac{2}{c}\frac{\partial u}{\partial t} - \beta\,\frac{c}{2}\int \frac{\partial^2 u}{\partial x^2}\,dt\right) = (\alpha+\beta)\frac{\partial^2 u}{\partial x^2} \tag{7}$$

With $\alpha = .5,\ \beta = .25$ and $\alpha = .478,\ \beta = .376$, (7) is called 45 degree and 65 degree approximation, respectively.

3 Migration by the operator splitting

With normalization of the time (t) by the wave speed $\frac{c}{2}$ and reverting the time, (5) is written as

$$\begin{pmatrix} u_t \\ \\ v_t \end{pmatrix} = \begin{pmatrix} 0 & 0 \\ \\ 0 & -\dfrac{\partial}{\partial z} \end{pmatrix} \begin{pmatrix} u \\ \\ v \end{pmatrix} + \begin{pmatrix} 0 & 1 \\ \\ \dfrac{1}{2}\dfrac{\partial^2}{\partial x^2} & 0 \end{pmatrix} \begin{pmatrix} u \\ \\ v \end{pmatrix}. \tag{8}$$

So, we apply the time splitting on $[t, t+\Delta t]$ of the Lie-Trotter form

$$(9) \qquad \begin{pmatrix} u_t \\ \\ v_t \end{pmatrix} = \begin{pmatrix} 0 & 0 \\ \\ 0 & -\dfrac{\partial}{\partial z} \end{pmatrix} \begin{pmatrix} u \\ \\ v \end{pmatrix}, \quad \begin{pmatrix} u_t \\ \\ v_t \end{pmatrix} = \begin{pmatrix} 0 & 1 \\ \\ \dfrac{1}{2}\dfrac{\partial^2}{\partial x^2} & 0 \end{pmatrix} \begin{pmatrix} u \\ \\ v \end{pmatrix}.$$

The first step of (9) is equivalent to the shift operation;

$$\begin{cases} v(t+\Delta t, x, z) = v(t, x, z-\Delta t), \quad z \geq \Delta t \\ \\ v(t+\Delta t, x, z) = \dfrac{\partial}{\partial t}\mathrm{SAS}(x, t+z), \quad z \in [0, \Delta t) \end{cases}$$

The second step of (9) is the one-D wave equation in x and is well-posed. In fact, let $\Omega = [-L, L] \times [0, 1]$ and $H^{1,x}(\Omega) = \{\phi \in L^2(\Omega) : \dfrac{\partial}{\partial x}\phi \in L^2(\Omega)\}$. Let $X_1 = H^{1,x}(\Omega) \times L^2(\Omega)$ be the Hilbert space equipped with

$$|(u, v)|^2_{X_1} = \int_\Omega (|\frac{\partial u}{\partial x}|^2 + 2|v|^2)\, dxdz.$$

Define the linear operator $\mathcal{A}_1$ on X_1 by

$$\mathcal{A}_1(u, v) = (v, \frac{1}{2}\frac{\partial^2 u}{\partial x^2})$$

with

$$dom(\mathcal{A}_1) = \{(u, v) \in X_1 : v \in H^{1,x}(\Omega),\ \frac{\partial^2 u}{\partial x^2} \in L^2(\Omega)$$

$$\text{with } \frac{\partial u}{\partial x}(\pm L, z) = 0\}$$

Then, $\mathcal{A}_1$ is dissipative and skew-adjoint on X_1 and thus generates a strongly continuous group on X_1. Hence, it is easy to show that if (u, v) is generated by (9) then

$$|(u, v)(t+\Delta t)|^2_{X_1} \leq |(u, v)(t)|^2_{X_1} + \int_t^{t+\Delta t} |\frac{\partial}{\partial t}\mathrm{SAS}(x, s)|^2\, dxds$$

and

$$|(u, v)(T)|^2_{X_1} \leq \int_0^T |\frac{\partial}{\partial t}\mathrm{SAS}(x, t)|^2\, dxdt.$$

Similarly, we can argue that (8) itself is well-posed, i.e., if we define the operator $\mathcal{A}$ on X_1 by

$$\mathcal{A}(u, v) = (v, div_{x,z}(\frac{1}{2}\frac{\partial u}{\partial x}, -v))$$

with

$$dom(\mathcal{A}) = \{(u, v) \in X_1 : v \in H^{1,x}(\Omega),\ div_{x,z}(\frac{1}{2}\frac{\partial u}{\partial x}, -v) \in L^2(\Omega) \text{ with } v(x, z) = 0,\ \frac{\partial u}{\partial x}(\pm L, z) = 0\},$$

then $\mathcal{A}$ is dissipative and generates a contractive, strongly continuous semigroup on X_1.

We fully discretize (9) and obtain

Algorithm I

$$\hat{v}_{i,j+1}^{n+1} = v_{i,j}^n, \;\; 1 \le j \le n \text{ with } \hat{v}_{i,0}^{n+1} = \frac{\mathrm{SAS}_i^{n+1} - \mathrm{SAS}_i^n}{\Delta t}$$

(10)

$$u_{\cdot,j}^{n+1} = (I + \frac{\tilde{c}^2}{2}H)^{-1}(u_{\cdot,j}^n + \Delta t \hat{v}_{\cdot,j}^{n+1}), \quad v_{\cdot,j}^{n+1} = \frac{u_{\cdot,j}^{n+1} - u_{\cdot,j}^n}{\Delta t}, \; 1 \le j \le \min(n, M)$$

where $u_{i,j}^n$ and $v_{i,j}^n$ represents the value of u and v at the grid-point $(i\Delta x, j\Delta z)$ at time $n\Delta t$, respectively. Here, $\Delta t = \Delta z$ and $\tilde{c} = \dfrac{\Delta z}{\Delta x}$, $H \in R^{N+1,N+1}$ is the tri-diagonal matrix defined by

$$(Hu)_i = -(u_{i+1} - 2u_i + u_{i-1}), \;\; 2 \le i \le N,$$

$$\text{and} \quad (Hu)_1 = -(u_2 - u_1), \quad (Hu)_{N+1} = u_{N+1} - u_N$$

and corresponds to the central difference approximation of $-\dfrac{\partial^2 u}{\partial x^2}$. Also, we used the implicit Euler scheme to integrate the second step (1-D wave equation in x). That is,

$$\frac{u_i^{n+1} - u_i^n}{\Delta t} = -\frac{1}{\Delta x^2}(Hu)_i, \quad \frac{v^{n+1} - \tilde{v}^n}{\Delta t} = u^{n+1}.$$

The number of operations at the n-th time step of (10) is of order $O(N \min(n, M))$. M is the number of the focusing step at each pixel (i, j) in cross-range direction x and if $j \ge M$, then $u_{i,j+1}^{n+1} = u_{i,j}^n$. Thus, the total operation is of order $O(MM^2)$.

For the wide angle equation (7) we define

$$F = \frac{2}{c}\frac{\partial u}{\partial t} - \beta\frac{c}{2}\int_0^t \frac{\partial^2 u}{\partial x^2}\, dt \quad \text{and} \quad v = \frac{2}{c}\frac{\partial u}{\partial t}.$$

It follows from (7) that

$$\frac{2}{c}\frac{\partial F}{\partial t} = (\frac{2}{c})^2\frac{\partial^2 u}{\partial t^2} - \beta\frac{\partial^2 u}{\partial x^2} = -\frac{\partial F}{\partial z} + \alpha\,\frac{\partial^2 u}{\partial x^2}$$

and

$$\frac{\partial}{\partial t}(v - F) = \frac{c}{2}\beta\,\frac{\partial^2 u}{\partial x^2}.$$

Thus, (7) is equivalent to

$$\frac{2}{c}\frac{\partial F}{\partial t} + \frac{\partial F}{\partial z} = \alpha\,\frac{\partial^2 u}{\partial x^2}$$

(11)

$$\frac{2}{c}\frac{\partial u}{\partial t} = (v - F) + F$$

$$\frac{2}{c}\frac{\partial}{\partial t}(v - F) = \beta\,\frac{\partial^2 u}{\partial x^2}.$$

With $\tilde{v} = v - F$, we use the three step splitting:

$$(12) \qquad \begin{cases} \dfrac{\partial F}{\partial t} + \dfrac{\partial F}{\partial z} = 0 \\ \dfrac{\partial u}{\partial t} = 0 \\ \dfrac{\partial \tilde{v}}{\partial t} = 0 \end{cases} \quad \begin{cases} \dfrac{\partial F}{\partial t} = 0 \\ \dfrac{\partial u}{\partial t} = \tilde{v} \\ \dfrac{\partial \tilde{v}}{\partial t} = \beta \dfrac{\partial^2 \tilde{v}}{\partial x^2} \end{cases} \quad \begin{cases} \dfrac{\partial F}{\partial t} = \alpha \dfrac{\partial^2 F}{\partial x^2} \\ \dfrac{\partial u}{\partial t} = F \\ \dfrac{\partial \tilde{v}}{\partial t} = 0 \end{cases}$$

If $\beta = 0$ then $\tilde{v} = 0$, $F = v$ and thus it reduces to the two-step splitting method (9). The first equation is accompanied by the boundary condition

$$F(t, x, 0) = \frac{\partial}{\partial t}\mathrm{SAS}(t, x) - \tilde{v}(t, x, 0).$$

Each step of (12) is a well-posed linear system as shown above and we can prove that (11) is well-posed. In fact, let $\Omega = [-L, L] \times [0, 1]$ and define the linear operator on $\mathcal{A}_2$ on $X_2 = L^2(\Omega) \times H^{1,x}(\Omega) \times L^2(\Omega)$ by

$$\mathcal{A}_2(F, u, \tilde{v}) = (-\frac{\partial F}{\partial z} + \alpha \frac{\partial^2 u}{\partial x^2}, \tilde{v} + F, \beta \frac{\partial^2 u}{\partial x^2})$$

with

$$dom(\mathcal{A}_2) = \{\frac{\partial}{\partial z} F \in L^2(\Omega), \text{ with } F(\cdot, 0) = 0 \text{ and}$$

$$\frac{\partial^2}{\partial x^2} u \in L^2(\Omega) \text{ with } \frac{\partial u}{\partial x}(\pm L, z) = 0, \frac{\partial}{\partial x}(\tilde{v} + F) \in L^2(\Omega)\}.$$

We equip X_2 with norm

$$|(F, u, \tilde{v})|^2_{X_2} = \int_\Omega (|\frac{\partial}{\partial x} u|^2 + \frac{1}{\alpha}|F|^2 + \frac{1}{\beta}|\tilde{v}|^2)\, dxdz$$

Then, $\mathcal{A}_2$ is dissipative, i.e.,

$$\begin{aligned} &(\mathcal{A}_2(F, u, \tilde{v}), (F, u, \tilde{v})) \\ &= \int_\Omega (\frac{\partial^2 u}{\partial x^2}(\tilde{v} + F) + \frac{\partial u}{\partial x}\frac{\partial}{\partial x}(\tilde{v} + F) - \frac{\partial F}{\partial z} F)\, dxdz \\ &= -\frac{1}{2}\int_{-L}^{L} |F(x, 1)|^2\, dx \le 0. \end{aligned}$$

Since $range(\mathcal{A}_2) = X_2$, $\mathcal{A}_2$ generates a strongly continuous, contraction semigroup on X_2. Similarly, we have the energy estimate

$$\int (|\frac{\partial}{\partial x} u(T)|^2 + \frac{1}{\alpha}|F(T)|^2 + \frac{1}{\beta}|\tilde{v(T)}|^2\, dxdz \le \int_0^T \int |F(t, x, 0)|^2\, dx\, dt.$$

Algorithm I is extended to integrate (12) as follows;

Algorithm II

$$\hat{F}^{n+1}_{i,j+1} = F^n_{i,j}, \;\; 1 \le j \le n \text{ with } \hat{F}^{n+1}_{i,0} = \frac{\mathrm{SAS}^{n+1}_i - \mathrm{SAS}^n_i}{\Delta t} - \tilde{v}^n_{i,0}$$

$$\hat{u}^{n+1}_{\cdot,j} = (I + \beta\tilde{c}^2 H)^{-1}(u^n_{\cdot,j} + \Delta t \hat{F}^{n+1}_{\cdot,j}), \quad F^{n+1}_{\cdot,j} = \frac{\hat{u}^{n+1}_{\cdot,j} - u^n_{\cdot,j}}{\Delta t}, \; 1 \le j \le \min(n, M)$$

$$u^{n+1}_{\cdot,j} = (I + \alpha\tilde{c}^2 H)^{-1}(\hat{u}^{n+1}_{\cdot,j} + \Delta t \tilde{v}^n_{\cdot,j}), \quad v^{n+1}_{\cdot,j} = \frac{u^{n+1}_{\cdot,j} - \hat{u}^{n+1}_{\cdot,j}}{\Delta t}, \; 1 \le j \le \min(n, M).$$

That is, we require double the operations for the integration of Algorithm II.

4 Advantages of the proposed methods

The frequency domain ω-k method based on Stolt's map [7] is the most efficient and accurate method for the homogeneous media due to the efficiency of fast Fourier transform. It also assumes a rectilinear sonar path.

We can use our proposed algorithms as a means to compensate the motion of sonar path. That is, let Γ be a curved sonar path and Γ_0 is a reference rectilinear path (z=0). Then we solve (5) or (7) on the domain enclosed by the boundaries Γ and Γ_0 with boundary value

$$u(t, x, z) = \mathrm{SAS}(t, x), \quad (x, z) \in \Gamma$$

In this way we have the mapped-SAS data $u(t, x, 0)$ at Γ_0 and then apply the $omega - k$ method for the rectangular domain Ω.

Our implementation (10) of the one-way wave equations is easily adjusted to the case of layered media $c = c(z)$ by varying the range increments Δz.

The proposed method can allow to localize the integration on sub-layered regions (assuming the homogeneous media). Also, we can integrate (5) or (7) in overlapped sub-domains in the cross-range (x) direction and then apply the superposition. This improves the efficiency of the proposed algorithms.

5 BV-type Regularization for Enhancement of SAS imaging

SAS imaging $s(x, z)$ may be altered by inhomogeneity of the field, sensor noise and irregularity of the sonar path and so on. We use the image enhancement technique based on BV-type reguralization [5].

Enhancement S of s minimizes

$$\int_\Omega |S-s|^2\,dxdz + \beta \int_\Omega \varphi(|\frac{\partial S}{\partial x}|^2 + |\frac{\partial S}{\partial z}|^2)\,dxdz \tag{12}$$

where

$$\beta > 0 \text{ is the regularization parameter}$$

and

$$Q(\phi) = \int_\Omega \varphi(|\nabla S|^2)\,dxdz \text{ defines the restoration energy.}$$

The followings summarize our findings in [5] on the enhancement based on(12);

- $\varphi(t^2) = t^2$ corresponds to the standard Gaussian filter and works well for a smooth image s.
- $\varphi(t^2) = t$ corresponds to the BV (nonlinear) filter and restores edges and flat regions of image s very well. But, it has significant stair-case effects.
- In order to deal with images with multi-scales of edges, flat, and smooth regions we developed an algorithm which uses

$$\varphi'(s) = \begin{cases} \frac{1}{\sqrt{s}} & s \in [1,\infty) \\ 1 & s \in [\delta, 1] \\ \frac{1}{\sqrt{s}} & s \in (0,\delta) \end{cases}$$

  It is based on the scale analysis and we demonstrated the applicability of the algorithm in [5].

- The necessary and sufficient condition of (12) is given by

$$-\beta\,\nabla\cdot(\varphi'(|\nabla S|^2)\nabla S) + S = s.$$

An efficient algorithm for finding S based on the fixed point iterate;

$$-\beta\,\nabla\cdot(\varphi'(|\nabla S^k|^2)\nabla S^{k+1}) + S^{k+1} = s$$

is developed and analyzed in [5] and is used in our test.

6 A Test

The algorithm is successfully applied to real data that are available to us via the Naval Surface Warfare Center (NSWC) and shows a promising capability. A full capability is going to be tested in the line of its advantages discussed in Section 4. In the following figures we show the raw SAS data, SAS imaging by algorithm (10), and the image enhanced by our enhancement algorithm. The last figure is produced by the most advanced implementation of ω-k method at NSWC. In the raw data returning echo signals are formed into a narrow imaging beam via synthetic aperture processing. The image area is of dimension 30m x 8m. The performance of our algorithms are comparable but we are improving it further by means of the blind de-convolution technique based on the independent component analysis.

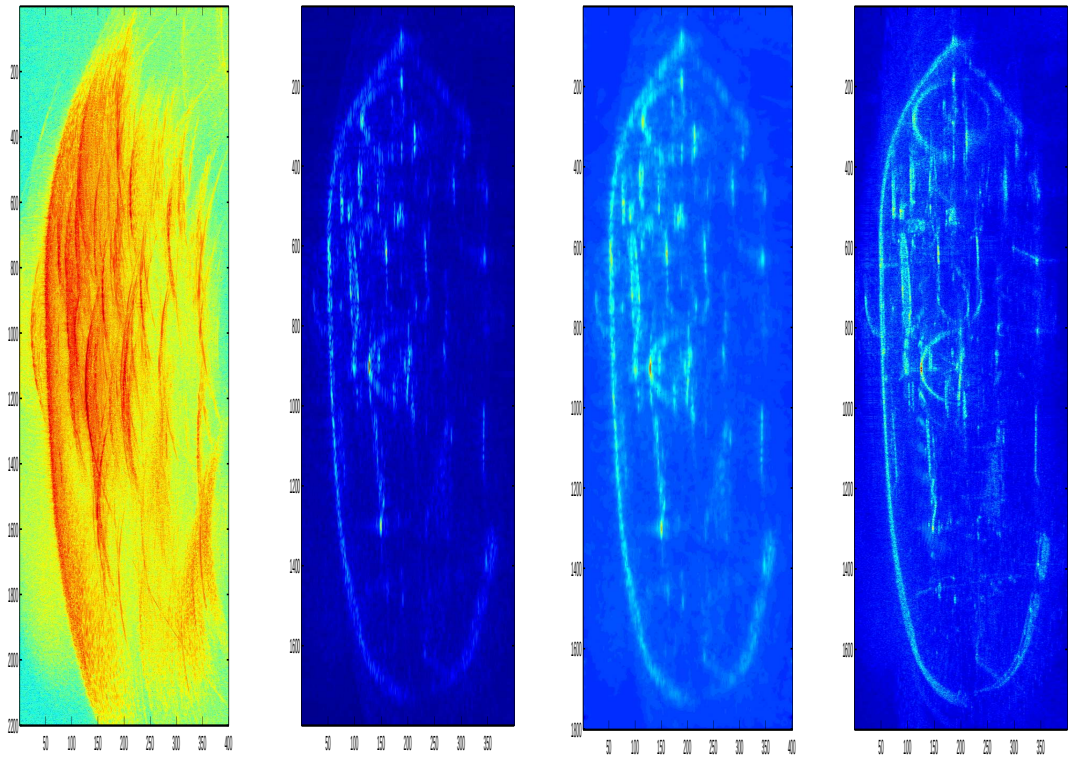

SAS Data One-Way Enhanced ω-k

References

[1] J.F. Clarebout, Coarse grid calculations of waves in inhomogeneous media with applications to delineation of complicated seismic structure, Geophysics, 35 (1970), 407-418.

[2] M.N. Guddati and A.H. Heidari, Migration with arbitrary wide-angle wave equations, Geophysics, 70 (2005), S61-S70.

[3] D.W. Hawkins, *Synthetic aperture imaging algorithms: with applications to wide bandwidth sonar*, Ph.D thesis, University of Canterbury, 1996.

[4] M.P. Hayes and P.T. Gough. Broad-band synthetic aperture sonar. IEEE Journal of Oceanic Engineering, 17 (1992), 80-94.

[5] K. Ito and K. Kunisch, BV-type Regularization methods for convoluted objects with edge-flat-grey scale, Inverse Probles 16 (2000), 909-928.

[6] M. Soumekhi, *Fourier Array Imaging*, Prentice Hall, Englewood Clifs, NJ, 1994.

[7] R.H. Stolt, Migration by Fourier transform, Geophysics, 43 (1978), 23-48.